

Blood flow simulation of left ventricle and aorta with translation motion

*Masashi Yamakawa¹, Yuto Yoshimi¹, Shinichi Asao² and Kyohei Tajiri¹

¹Faculty of Mechanical Engineering, Kyoto Institute of Technology, Japan.

²Department of Mechanical Engineering, College of Industrial Technology, Japan

*Presenting and corresponding author: yamakawa@kit.ac.jp

Abstract

To specify causes of heart diseases, it is very important to understand a blood flow state in an aorta. In this paper, the blood flow which pushed out to the aorta according to a contraction motion of a left ventricle was simulated. To express its complicated shape and the motion, the unstructured moving grid finite volume method was adopted. In this method, the control volume is defined for a space time unified domain. Not only a physical conservation law but also a geometric conservation law is satisfied in this approach. Then high accurate computation is conducted under the method. The left ventricle expands and contracts, at the same time, the ventricle and the aorta perform a translational motion. The model of its motion captured from the computed tomography images is also introduced to this computation. The result of flow calculation in left ventricle matches with the measurement result qualitatively. A flow in an aorta has a dramatic shift on its style in the contraction process of left ventricle. We also succeeded to capture its shift on our result of the flow in the aorta. Then, the tendency of the flow also matches with the computation and measurement result of others. Furthermore, the complicated vortex structure in the left ventricle was shown as the results of the simulation. Thus, the validity of the computational method and the possibility of calculation for capturing detail flows in left ventricle and aorta were shown in this paper.

Keywords: Computational fluid dynamics, Blood flow simulation, Left ventricle, Aorta

Introduction

There are a lot of threat serious or life threatening disease in a heart and vascular diseases, for example arteriosclerosis or an aneurysm. It is known from clinical observation that the heart and vascular diseases often appear at bifurcation or flexure of thick blood vessel. Thus, the relation between the origin of the heart disease and blood flow has been pointed out. Then, various hypotheses regarding the fluid dynamics factor of the heart and vascular diseases have been made. To prove the validity of the hypotheses, flows in a heart or blood vessel have been studied through the method of experimentation or numerical simulation. Ku et al. [1] made a measurement the intimal thickening generated at the branching part of the human arteria carotis communis, as they were focused on the relations between the intimal thickening of an artery and the blood flow. Then, it was shown that the intimal thickening has a correlation with the time fluctuation of shear force measured on a glass tube flow made from specimens of blood vessel. Fukushima et al. [2] created a visualization of blood flow using the real blood vessel taken out from the body. The real blood vessel is made transparent by salicylic acid. Then, they determined whether vortex tube exist at the bifurcation of the blood vessel. While, by multi scale computing using the finite element method, Sugiura et al. [3] created the numerical heart in the supercomputer although it took a huge cost.

And now, the aorta connected to the left ventricle is comprised of three parts as the aorta ascendens expanding upward, the aortic arch taking a bend, and the aorta descendens expanding downward. Then, the three principal branched blood vessels expand from the

aortic arch. The blood current in the aorta behaves like an intermittent flow which alternates start and stop flow, because the aortic valve located between the aorta and the left ventricle has to alternate close and open to occur the flow from the left ventricle to the aorta. The complicated flow phenomenon in the aorta is created from the geometric feature and the pulsatility of the aorta. Then, it is very interesting from the hemodynamic standpoint regarding the relation between the origin of the heart disease and the factor of the fluid dynamics. It is at an increased risk for developing of the disease at the left ventricle and the aorta. Furthermore, it would become more serious when it develops. From the point of the view, a lot of researches [4] of the left ventricle and the aorta have been conducted. The objective of our paper is to develop an efficient computation method for flows of the left ventricle and the aorta with satisfying the expression of the complicated shapes and the function. To calculate more accurately, not only expansion and contraction of the left ventricle but also translational motion of the aorta is adopted as the motion for computation. In particular, to satisfy a physical conservation law and a geometric conservation law, the unstructured moving grid finite volume method [5][6] is adopted. In this method, a control volume is defined for a space time unified domain. The method made it possible to compute accurately for motion of the left ventricle and the aorta. Furthermore, the unstructured mesh approach was also able to express such the complicated shape. Then, the computation was carried out under the OpenMP parallel environment [7].

Numerical Approach

Governing Equations

As governing equations, the continuity equation and the Navier-Stokes equations for incompressible flows are adopted and written as follows:

$$\nabla \cdot \mathbf{q} = 0, \quad (1)$$

$$\frac{\partial \mathbf{q}}{\partial t} + \frac{\partial \mathbf{E}_a}{\partial x} + \frac{\partial \mathbf{F}_a}{\partial y} + \frac{\partial \mathbf{G}_a}{\partial z} = - \left(\frac{\partial \mathbf{E}_p}{\partial x} + \frac{\partial \mathbf{F}_p}{\partial y} + \frac{\partial \mathbf{G}_p}{\partial z} \right) + \frac{1}{\text{Re}} \left(\frac{\partial \mathbf{E}_v}{\partial x} + \frac{\partial \mathbf{F}_v}{\partial y} + \frac{\partial \mathbf{G}_v}{\partial z} \right), \quad (2)$$

where \mathbf{q} is the velocity vector, \mathbf{E}_a , \mathbf{F}_a , and \mathbf{G}_a are advection flux vectors in the x , y , and z direction, respectively, \mathbf{E}_v , \mathbf{F}_v , and \mathbf{G}_v are viscous-flux vectors, and \mathbf{E}_p , \mathbf{F}_p , and \mathbf{G}_p are pressure terms. The elements of the velocity vector and flux vectors are

$$\begin{aligned} \mathbf{q} &= \begin{bmatrix} u \\ v \\ w \end{bmatrix}, \quad \mathbf{E}_a = \begin{bmatrix} u^2 \\ uv \\ uw \end{bmatrix}, \quad \mathbf{F}_a = \begin{bmatrix} uv \\ v^2 \\ vw \end{bmatrix}, \quad \mathbf{G}_a = \begin{bmatrix} uw \\ vw \\ w^2 \end{bmatrix}, \quad \mathbf{E}_p = \begin{bmatrix} p \\ 0 \\ 0 \end{bmatrix}, \\ \mathbf{F}_p &= \begin{bmatrix} 0 \\ p \\ 0 \end{bmatrix}, \quad \mathbf{G}_p = \begin{bmatrix} 0 \\ 0 \\ p \end{bmatrix}, \quad \mathbf{E}_v = \begin{bmatrix} u_x \\ v_x \\ w_x \end{bmatrix}, \quad \mathbf{F}_v = \begin{bmatrix} u_y \\ v_y \\ w_y \end{bmatrix}, \quad \mathbf{G}_v = \begin{bmatrix} u_z \\ v_z \\ w_z \end{bmatrix}, \end{aligned} \quad (3)$$

where u , v , and w are the velocity components of the x , y , and z directions, respectively, and p is pressure. The subscripts x , y , and z indicate derivatives with respect to x , y , and z , respectively. Here, Re is the Reynolds number.

The Unstructured Moving-Grid Finite-Volume Method

In this simulation, expansion and contraction of the left ventricle and translation motion of the aorta are expressed using moving mesh approach. To assure a geometric conservation law in moving mesh, a control volume is defined in a space-time unified domain. For the discretization, Eq. (2) can be written in divergence form as

$$\tilde{\nabla} \cdot \tilde{\mathbf{F}} = \mathbf{0}, \quad (4)$$

where

$$\tilde{\nabla} = \begin{bmatrix} \frac{\partial}{\partial x} \\ \frac{\partial}{\partial y} \\ \frac{\partial}{\partial z} \\ \frac{\partial}{\partial t} \end{bmatrix}, \quad \tilde{\mathbf{F}} = \begin{bmatrix} \mathbf{E}_a + \mathbf{E}_p - \frac{1}{\text{Re}} \mathbf{E}_v \\ \mathbf{F}_a + \mathbf{F}_p - \frac{1}{\text{Re}} \mathbf{F}_v \\ \mathbf{G}_a + \mathbf{G}_p - \frac{1}{\text{Re}} \mathbf{G}_v \\ \mathbf{q} \end{bmatrix}. \quad (5)$$

The flow variables are defined at the center of the cell in the (x, y, z) space, as the approach is based on a cell-centered finite volume method. Thus, the control volume becomes a four-dimensional polyhedron in the (x, y, z, t) -domain. For the control volume, Eq. (4) is integrated using the Gauss theorem and written in surface integral form as:

$$\int_{\tilde{\Omega}} \tilde{\nabla} \cdot \tilde{\mathbf{F}} d\tilde{V} = \oint_{\partial\tilde{\Omega}} \tilde{\mathbf{F}} \cdot \tilde{\mathbf{n}}_u d\tilde{S} \approx \sum_{l=1}^6 (\tilde{\mathbf{F}} \cdot \tilde{\mathbf{n}})_l = \mathbf{0} \quad (6)$$

Here, $\tilde{\mathbf{n}}_u$ is an outward unit vector normal to the surface, $\partial\tilde{\Omega}$, of the polyhedron control volume $\tilde{\Omega}$, and $\tilde{\mathbf{n}} = (\tilde{n}_x, \tilde{n}_y, \tilde{n}_z, \tilde{n}_t)_l$, ($l=1, 2, \dots, 6$) denotes the surface normal vector of control volume, and its length is equal to the boundary surface area in four-dimensional (x, y, z, t) space. The upper and bottom boundary of the control volume ($l = 5$ and 6) are perpendicular to the t -axis, and therefore they have only the \tilde{n}_t component, and its length corresponds to the volume of the cell in the (x, y, z) -space at time t^n and t^{n+1} , respectively.

Computational Model and Conditions

Geometric Model of Left Ventricle and Aorta

The function of the left ventricle is draining blood to the aorta like a pump. The mitral valve and the aortic valve are put on the inlet and the outlet of the ventricle, respectively. The shape of the left ventricle is structured, as shown Fig. 1. Bothe of the diameter of blood vessels at the mitral valve and the aortic valve are 3.0cm. The length from the base of heart to the cardiac apex is 7.8cm at lumen maximum volume. The cross-section shape of the left ventricle is ellipse. Then, the ratio of the major axis and minor axis on the ellipse is 5 to 4.

While, the aorta is comprised of three parts which are the ascending aorta expanding upward, the aortic arch taking a bend, and the descending aorta expanding downward. Furthermore, the three principal branched blood vessels which are called innominate artery, left common carotid artery and left subclavian artery expand from the aortic arch. Then the aortic arch itself curves three-dimensionally. In other words, the central axis of the aortic arch is not on a plane surface. Thus, the aorta is complicated shape with bending, bifurcation and three-

dimensional torsion. In this paper, the shape of the aorta model is created, as shown Fig. 2. Then, Fig. 3 shows aortic arch with three-dimensional curve around the bifurcation points.

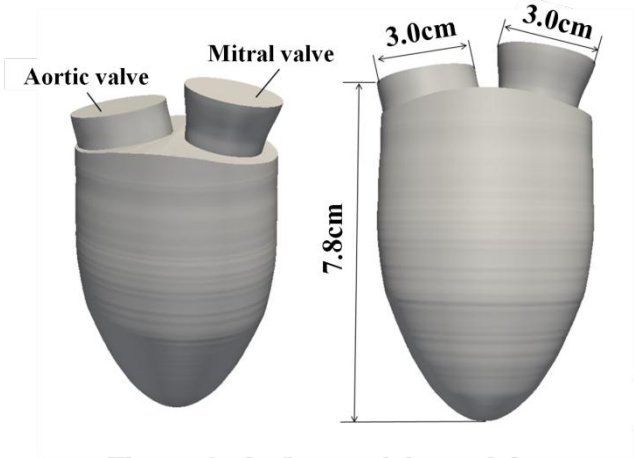


Figure 1. Left ventricle model

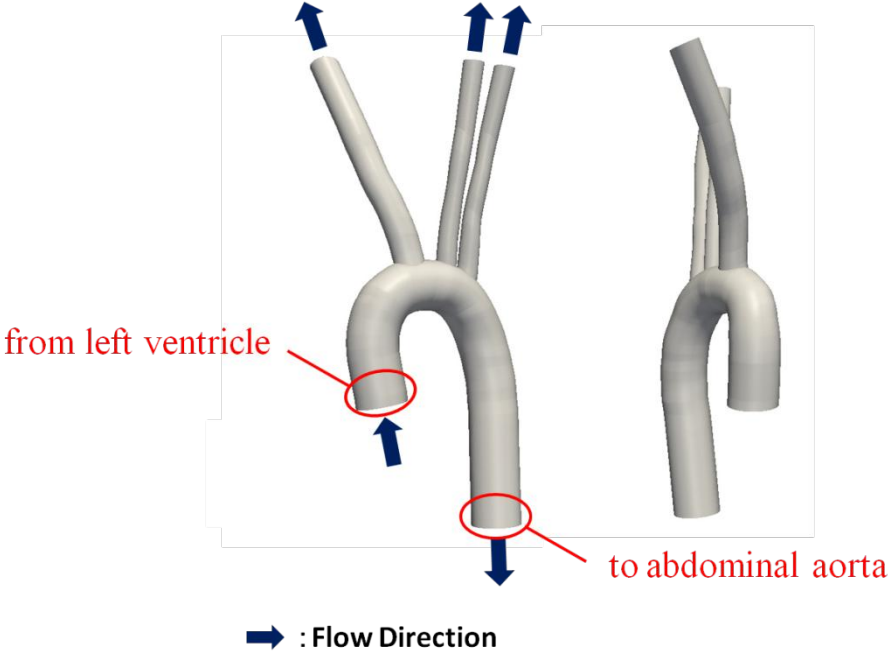


Figure 2. Aorta model

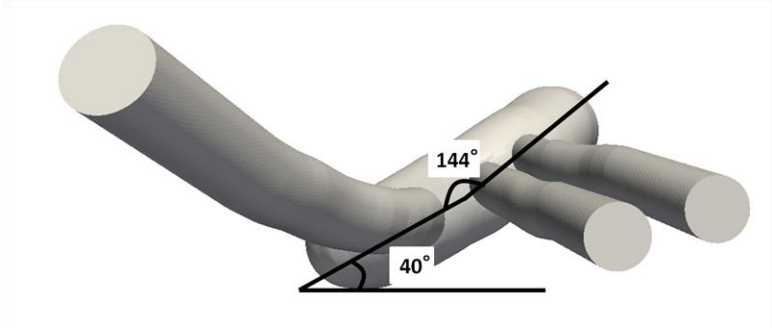


Figure 3. Angle of torsion at aortic arch from top view

Motions of Left Ventricle and Aorta

The left ventricle is draining blood to the aorta by expansion and contraction. Then the heart rate is determined the systole and diastole of the heart. Then, a period from starting point to the next starting point of heart rate is called the cardiac cycle. If a pulse rate is 60bpm, one cardiac cycle would be 1.0sec. Then, it is classified 0.49sec as the systole and 0.51sec as the diastole. The history of the left ventricle cavity volumetric change in one cardiac cycle is shown in Fig. 4. The expansion and contraction using moving mesh at the simulation are expressed under the history.

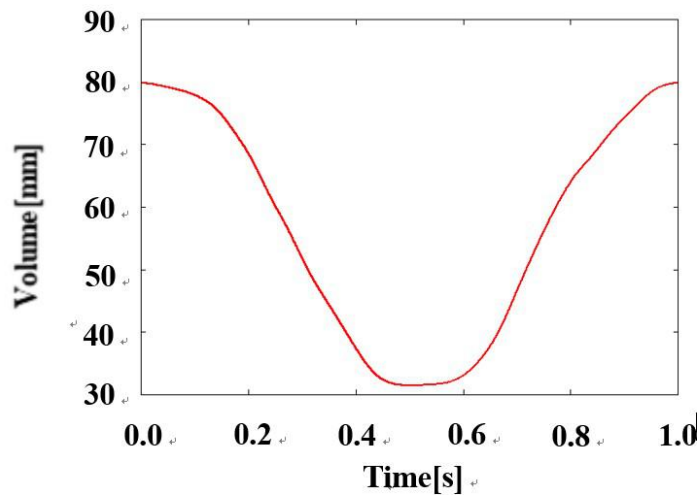


Figure 4. History of left ventricle volumetric change

Fig. 5 shows the computed tomography images of the left ventricle and the aorta [8]. The dark black line is a catheter injecting a contrast medium. The figure on the left is a front view of a human and the figure on the right is a side view.

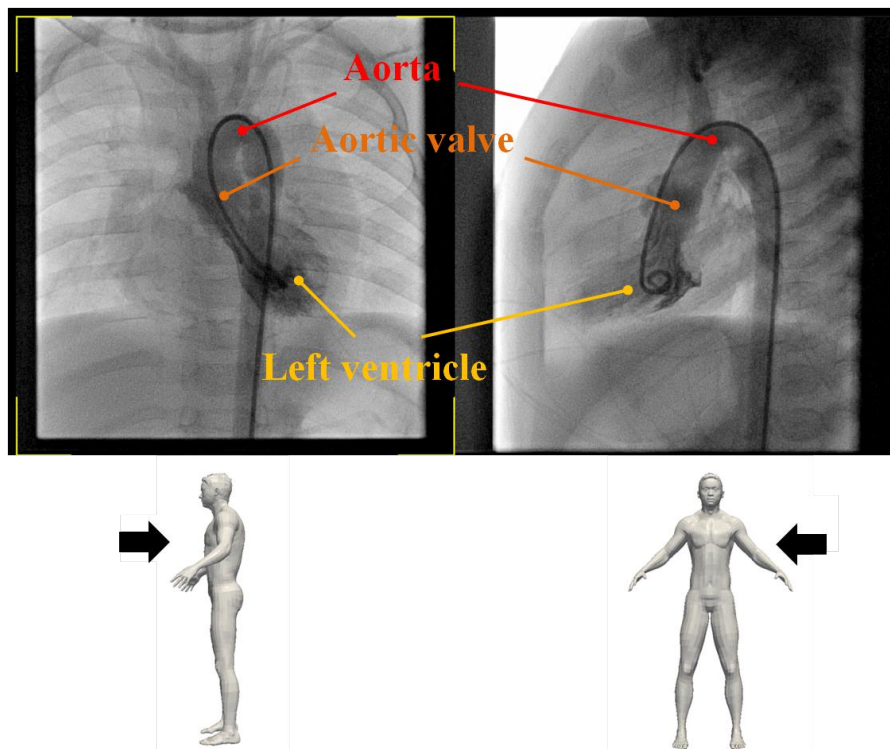


Figure 5. CT images of left ventricle and aorta (left: front view, right; side view)

Fig. 6 shows the CT images at the maximum volume of the left ventricle and Fig. 7 shows at the minimum one. On both figures, the red line indicates the point of the aortic valve at the maximum one. Then, the blue line indicates at the minimum one. From these figures, the translation motion of the position of the aortic valve is confirmed from the figures. Then, we can see the motion within a broader range from the left ventricle to the descending aorta. The motion can affect to the blood flow since the acceleration of the motion is relatively high. Thus, in this computation, the motion is introduced.

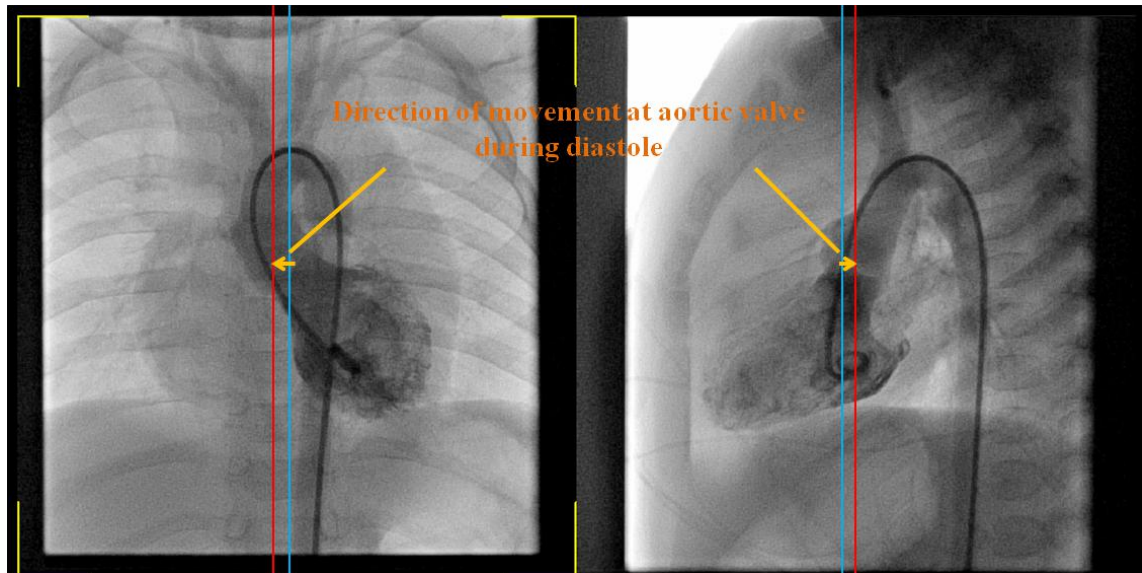


Figure 6. CT image at maximum volume of ventricle (left: front view, right; side view)

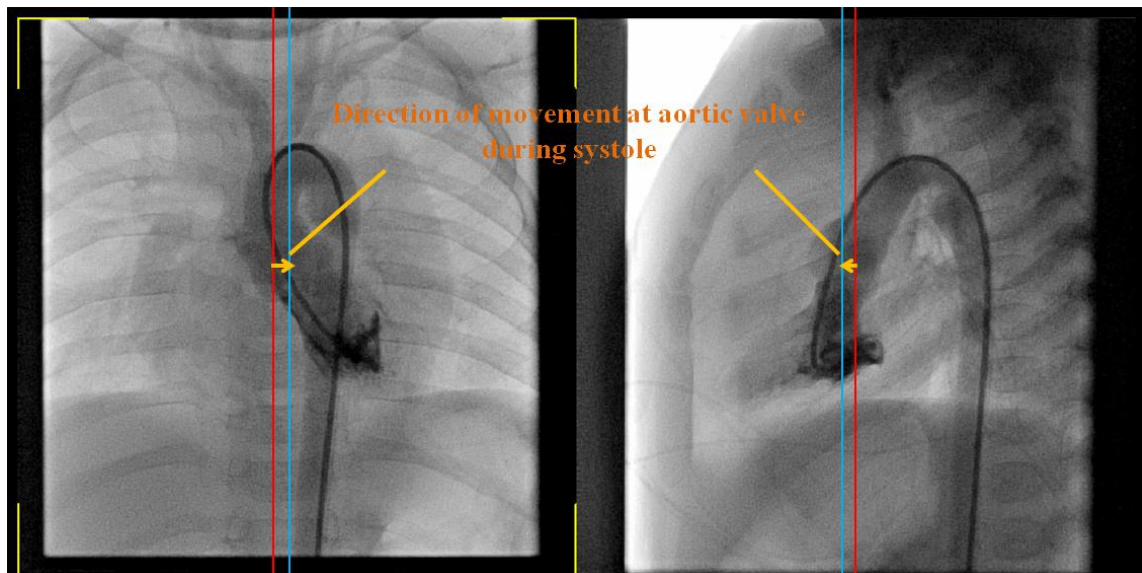


Figure 7. CT image at minimum volume of ventricle (left: front view, right; side view)

To know the length of the translation motion, the CT images are used. Several points are put on the images as shown in Fig. 8. These points correspond to the points at the computational model as shown in Fig. 9. The detail travel lengths are calculated using the height of the left ventricle as reference length L . Conducting the measurement by two aspects, the translation motion is estimated as three-dimensional movement.

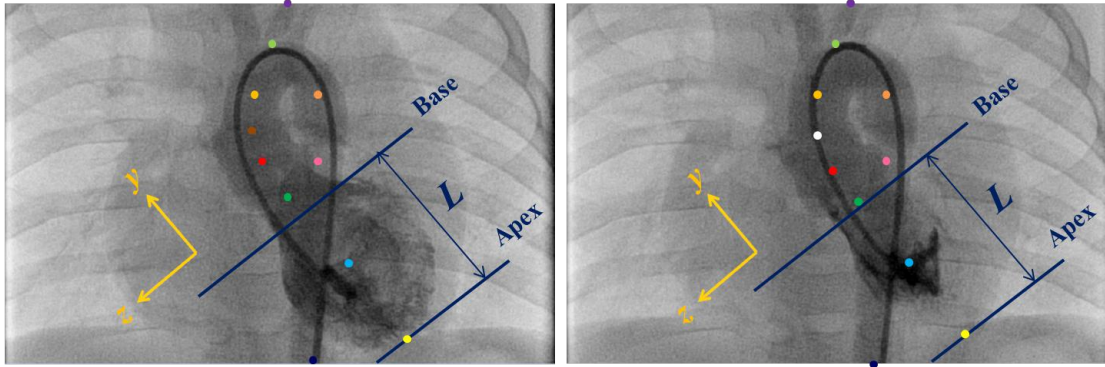


Figure 8. Measurement length of translation motion from CT image (left: at maximum volume, right; at minimum volume)

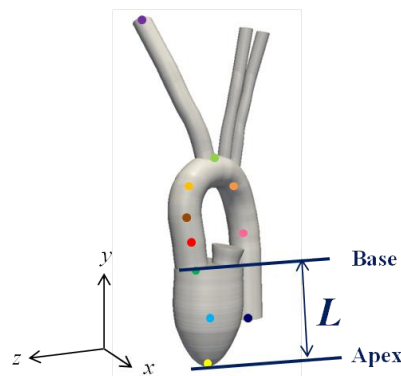


Figure 9. Corresponding points on computational model

Computational Conditions

The computational mesh is generated by MEGG3D [9] using tetrahedral and prism elements. The total number of the elements are 2,777,089. The heart rate is 60bpm, and the Reynolds number is 2,030. As an initial condition, pressure $p = 0$ and velocity for x, y, z directions $u = v = w = 0$ are obtained for all elements. In the cardiac diastole, the mitral valve is open and the aortic valve is closed completely. Then, the velocity at the mitral valve is given as a linear extrapolation and pressure is fixed as $p = 0$. While, in the cardiac systole, the mitral valve is closed and the aortic valve is open completely. These open and closing motion are conducted instantly. On the four exit of blood vessels, velocity is determined as a linear extrapolation and pressure is zero. The velocity on all walls of the left ventricle and the aorta is given the moving velocity decided expansion, contraction and translation motion.

Computational Results

Verification of the validity for the Computation

To verify the validity for the computational approach, results of the flows inside the left ventricle and the aortic arch are evaluated. Fig. 10 shows streamlines in the left ventricle at the third cardiac diastole from starting this calculation. By expansion of the left ventricle, the blood inflow through the mitral valve is seen. Then, we can confirm that the flow makes two vortexes. One is generated on the center of the left ventricle, which is larger than another one. Another is created between mainstream and the wall. The relatively large vortex is also seen in the measurement results of flow in the left ventricle by Kilner et al. as shown in Fig. 11.

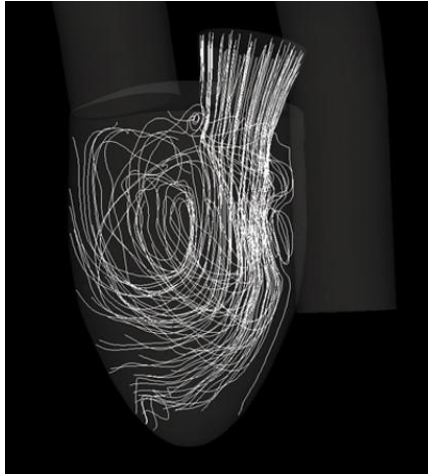


Figure 10. Streamlines in left ventricle on this computation result

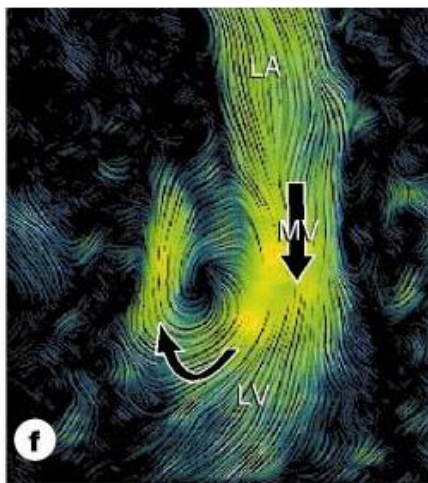
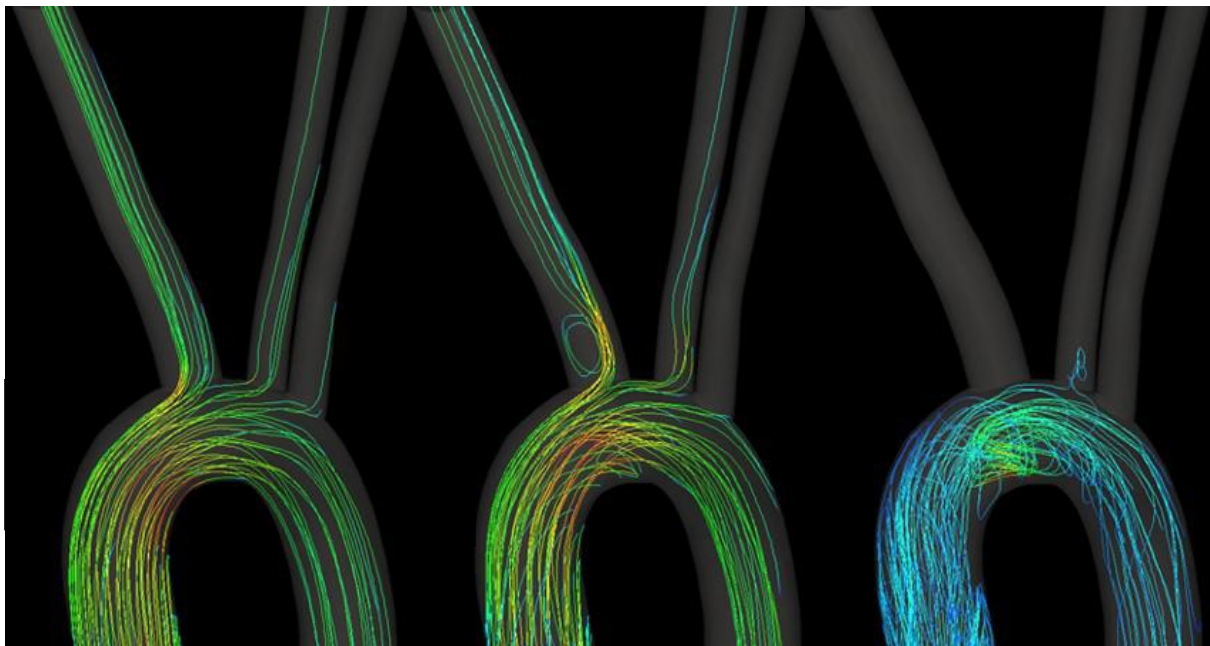


Figure 11. Measurement result of flow in left ventricle



**Figure 12. Streamline in aorta of the computation
(left: in early systole, center: in mid to late systole, right: in end systole)**

Fig. 12 shows streamlines in the aorta at the third cardiac systole from starting this calculation. In this figure, left one is in early systole, centered one is in mid to late systole, and right one is in end systole. In the early systole, a strong flow along the aortic arc from the left ventricle is seen. In the mid to late systole, a spiral flow along the mainstream is confirmed. Then, small vortex is generated at the entrance of the innominate artery. In the end systole, mainstream itself becomes weak and circulating flow along the aortic wall. Then, we can hardly see flows in the tributary. These results are also compared with other computation and measurement results. The computational results by Wada are shown in Fig. 13, and the measurement results by Kilner et al. are shown in Fig. 14. The tendencies of our computation results on each systole are seen in the other computation and measurement results.

Comparing with other computation and measurement results of flows inside the left ventricle and the aorta, the qualitative correspondences are seen in both case. Thus, the validity of the computational approach is confirmed.

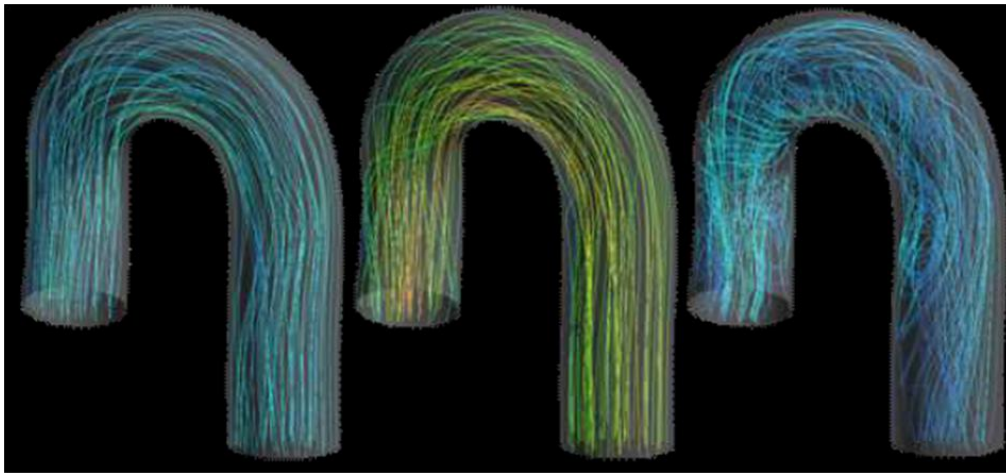


Figure 13. Streamline in aortic arch computed by Wada (left: in early systole, center: in mid to late systole, right: in end systole)

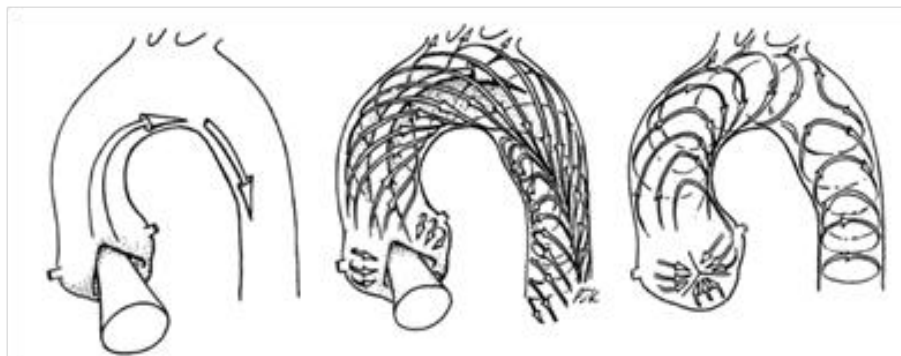


Figure 14. Measurement results in aortic arch by Kilner (left: in early systole, center: in mid to late systole, right: in end systole)

Blood Flow in Left Ventricle

The isosurface of Q criterion in the left ventricle at $t = 22.0, 23.0, 24.0, 25.0, 26.0$ and 27.0 are shown in Fig. 15. These are from in the third early systole to the third in the mid to late systole. Vortex structures generated by the cardiac beat from the second period remain in the left ventricle. Into the domain, the inflow of blood with generating the ring-shaped vortex tube from the mitral valve is seen. The vortex tube is collapsing according to a decrease in the inflow of blood from the mitral valve. Then it becomes a complicated vortex structure and

spreads in the left ventricle. Thus, the possibility of calculation for capturing detail flows in left ventricle is shown.

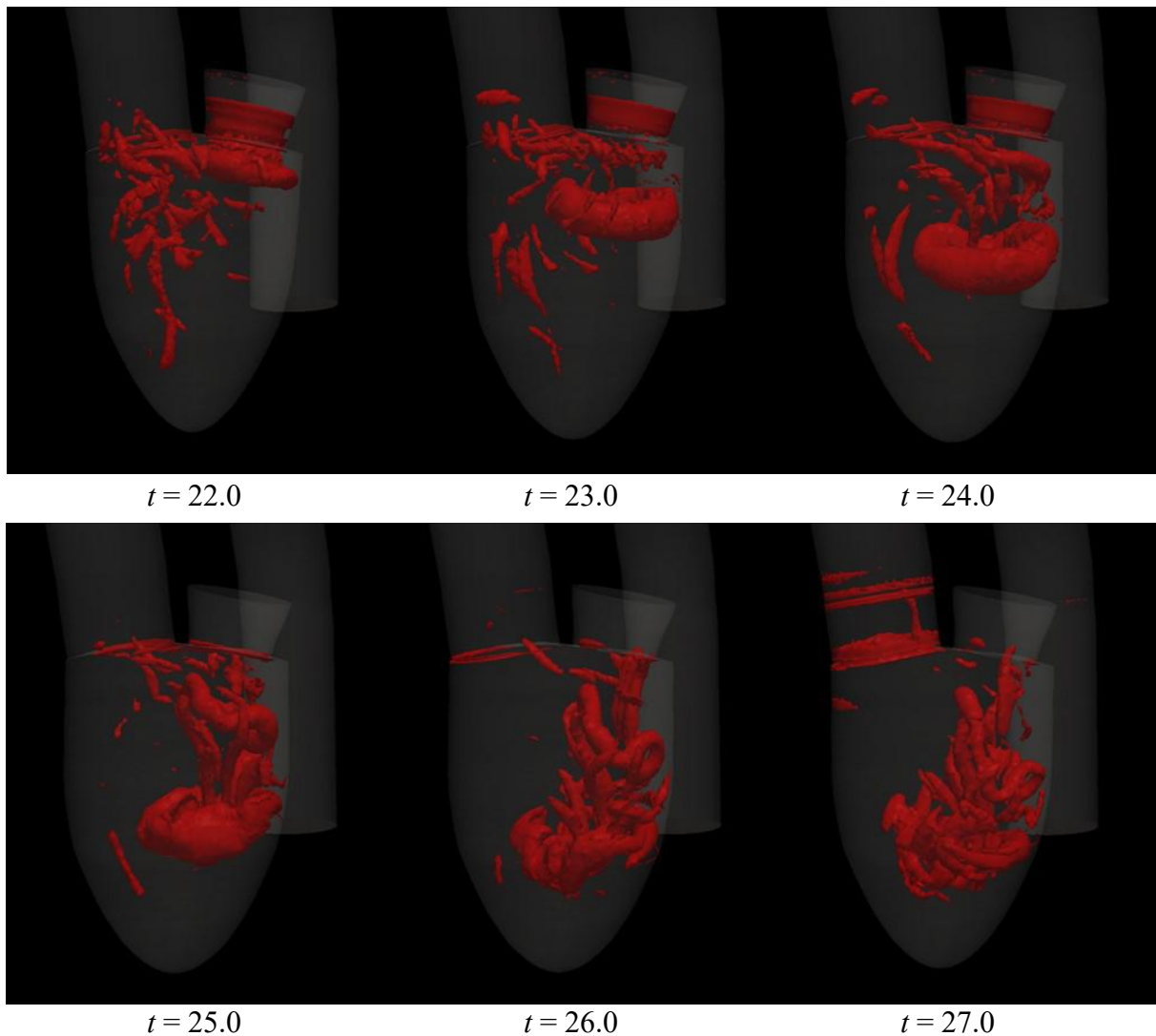


Figure 15. Isosurface of Q criterion in left ventricle ($t = 22.0$ to 27.0)

Conclusions

To construct the computational approach for specifying cause of heart diseases, blood flows in the left ventricle and the aorta were calculated. For high order accurately, the unstructured moving-grid finite-volume method was adopted. Furthermore, not only the expansion of contraction of the left ventricle but also translation motion of the aorta which is captured from the computed tomography images was adopted in this paper. From the results of the flow in the left ventricle compared with measurement result, the large vortex is seen. Furthermore, the flows in the aorta were estimated using the other computation and measurement results. As the tendencies on each systole are seen in both results, the qualitative correspondences are confirmed. Thus, the validity of the computational approach is shown. In the computation for blood flows inside of the left ventricle at the diastole, complicated vortex structures are captured by the approach. Thus, the possibility to computed and specify the cause of the diseases was shown.

Acknowledgments

This publication was subsidized by JKA through its promotion funds from KEIRIN RACE and by JSPS KAKENHI Grant Number 16K06079.

References

- [1] Ku, D., Giddens, et al, (1985) Pulsatile flow and atherosclerosis in the human carotid bifurcation. Positive correlation between plaque location and low oscillating shear stress., *Arteriosclerosis* Vol.5, 293-302
- [2] Fukushima, T. et al. (1982) The horseshoe vortex: A secondary flow generated in arteries with stenosis, bifurcation, and branching, *Biorheology* Vol.19, 143-154.
- [3] Sugiura, S., et al. (2012) Multi-scale simulations of cardiac electrophysiology and mechanics using the University of Tokyo heart simulator, *Progress in Biophysics and Molecular Biology*, 2012 Oct-Nov;110(2-3), 380-389
- [4] Liang, F., et al. (2007) A multi-scale computational method applied to the quantitative evaluation of the left ventricular function, *Computers in Biology and Medicine*, Vol.37, 700-715
- [5] Yamakawa, M., et al. (2012) Numerical Simulation for a Flow around Body Ejection using an Axisymmetric Unstructured Moving Grid Method, *Computational Thermal Sciences*, Vol.4, No.3, 217-223.
- [6] Yamakawa, M., et al. (2017) Numerical Simulation of Rotation of Intermeshing Rotors using Add-ed and Eliminated Mesh Method, *Procedia Computer Science* 108C, 1883-1892.
- [7] Yamakawa, M., et al. (2011) Domain decomposition method for unstructured meshes in an OpenMP computing environment, *Computers & Fluids*, Vol. 45, pp.168-171.
- [8] Fukui, T., et al. (2017) Influence of geometric changes in the thoracic aorta due to arterial switch operations on the wall shear stress distribution, *Open Biomedical Engineering Journal*, 11, 9-16.
- [9] Ito, Y. (2013) Challenges in Unstructured Mesh Generation for Practical and Efficient Computational Fluid Dynamics Simulations, *Computers and Fluids*, 85, 47-52.